Published online 19 September 2006 *Nucleic Acids Research, 2006, Vol. 34, No. 18* ***5039–5051***
doi:10.1093/nar/gkl644

The bipartite architecture of the sRNA in an archaeal box C/D complex is a primary determinant of specificity

John W. Hardin and Robert T. Batey*

Department of Chemistry and Biochemistry, University of Colorado, Boulder, CO 80309, USA

Received July 28, 2006; Accepted August 21, 2006

ABSTRACT

The archaeal box C/D sRNP, the enzyme responsible for 2′-*O*-methylation of rRNA and tRNA, possesses a nearly perfect axis of symmetry and bipartite structure. This RNP contains two platforms for the assembly of protein factors, the C/D and C′/D′ motifs, acting in conjunction with two guide sequences to direct methylation of a specific 2′--hydroxyl group in a target RNA. While this suggests that a functional asymmetric single-site complex complete with guide sequence and a single box C/D motif should be possible, previous work has demonstrated such constructs are not viable. To understand the basis for a bipartite RNP, we have designed and assayed the activity and specificity of a series of synthetic RNPs that represent a systematic reduction of the wild-type RNP to a fully single-site enzyme. This reduced RNP is active and exhibits all of the characteristics of wild-type box C/D RNPs except it is nonspecific with respect to the site of 2′-*O*-methylation. Our results demonstrate that protein–protein crosstalk through Nop5p dimerization is not required, but that architecture plays a crucial role in directing methylation activity with both C/D and C′/D′ motifs being required for specificity.

INTRODUCTION

RNA is often modified in the cell in order for it to achieve full biological function. Currently, about 100 distinct types of modification have been identified (1). While most of these are exclusively observed in tRNA (2), other functional RNAs are also modified (3–6). The importance of these modifications has become increasingly clear since the discovery that the two most common modification types in rRNA, pseudouridylation and 2′-*O*-methylation, cluster around the functional regions of the ribosome (7–9) suggesting that RNA modification may encourage proper folding (10,11) and structural stabilization (12) *in vivo*. Although biochemical data has supported this role in a number of cases (13), other significant functions for RNA modification are continually emerging.

Box C/D ribonucleoprotein (RNP) complexes act as RNA guided site-specific 2′-*O*-methyltransferases in archaea and eukaryotes (14,15). In archaea, these complexes are referred to as small RNP complexes (sRNPs). This RNP specifically methylates a 2′-hydroxyl in an RNA target with the site of methylation being the nucleotide paired to the guide sequence five bases upstream from either the D or the D′ box motif (16,17) (Figure 1a). The archaeal box C/D RNA contains C′ and D′ motifs in the middle of the RNA that generally conform to the box C/D consensus sequence (18) and two guide sequences of about 12 nt (19). This architecture means that the box C/D complex is capable of site-specifically methylating two unique RNA targets with methylation directed off of either the D or D′ box (Figure 1a).

The archaeal box C/D complex requires only three proteins for activity (20): L7Ae, which is also a ribosomal protein (21,22), fibrillarin and the Nop56/Nop58 homolog Nop5p. L7Ae binds both box C/D and the C′/D′ motifs (23), which respectively comprise kink-turn (24) or k-loop structures (25) to initiate the assembly of the RNP (26,27). Fibrillarin performs the transfer of the methyl group from the cofactor S-adenosylmethionine (SAM) to the target RNA (28–30). This reaction requires the precise positioning of the active site of fibrillarin over the specific 2′-hydroxyl group to be methylated. Interestingly, while fibrillarin methylates this functional group in the context of a Watson–Crick base paired helix (guide/target), it has little dsRNA binding activity by itself (23,30,31). This implies that its active site must be precisely positioned through interactions with the other components of the RNP.

Box C/D complexes possess a distinct but imperfect axis of symmetry (Figure 1a). While archaeal and eukaryal box C/D complexes are extremely similar in their structure and sequence conservation, this symmetry is more explicit in archaea where there is: (i) less deviation of the C′/D′ motif from the consensus box C/D sequence, (ii) the presence of a single Nop56/Nop58 homolog that is proposed to form an $\alpha_2\beta_2$ tetramer with fibrillarin further reflecting a 2-fold symmetry (32), (iii) less guide sequence length variability (19)

*To whom correspondence should be addressed. Tel: +1 303 735 2159; Fax: +1 303 735 1347; Email: robert.batey@colorado.edu

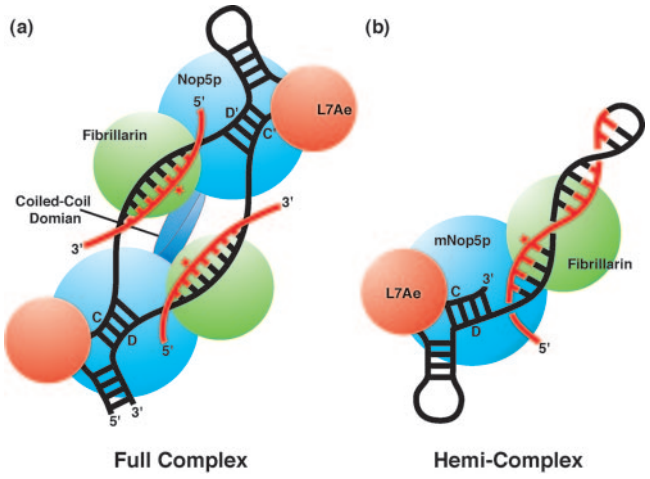

Figure 1. (**a**) Model of the full box C/D sRNP complex. (**b**) Model of the box C/D sRNP hemi-complex. L7Ae (red), Nop5p or mNop5p (blue) and fibrillarin (green).

and (iv) a more symmetric assembly of protein components onto the box C/D RNA (23,33–35). However there is still debate over the exact composition of the functional complex. A recent study (36) presents compelling evidence that the $\alpha_2\beta_2$ *Archaeoglobus fulgidus* Nop5p/fibrillrin tetramer observed in a crystal structure (32) may not be representative of the majority of archaeal box C/D RNPs. Instead, these proteins appear to be a functional heterodimer, with the coiled coil domain being essential for RNP function but not for mediating Nop5p dimerization (36).

The conserved symmetry of this RNP led us to question the functional purpose of the bipartite architecture in box C/D complexes. If proper positioning of fibrillarin over the site of methylation is solely accomplished through interaction with proteins anchored to either the box C/D or C′/D′ motifs, then it would seem as if an active complex could be assembled using a single box C/D motif and guide sequence. To understand how the bipartite arrangement relates to activity and specificity we have designed a series of complexes representing intermediaries between a minimal asymmetric RNP and the wild-type enzyme. These constructs allowed us to assess the functional contributions of various aspects of box C/D architecture by building towards the full wild-type complex and looking for restoration of wild-type behavior at each step. This approach revealed an active monomeric enzyme exhibiting most of the characteristics of wild-type enzyme except that it is a highly nonspecific methyltransferase. We also found that protein–protein cross talk through Nop5p dimerization is not required for specificity or activity. Significantly, other constructs revealed that the RNA architecture plays a crucial role in site-specifically directing methylation activity, with both the box C/D and C′/D′ motifs being required to achieve modification of the correct 2′-hydroxyl group.

MATERIALS AND METHODS

Protein expression and purification

The gene encoding L7Ae (GI 7440708) was amplified from *Pyrococcus horikoshii* genomic DNA by PCR and cloned into pET15b (Novagen) using standard techniques (37). L7Ae was expressed in Rosetta (DE3)/pLysS cells induced with 1 mM isopropyl-β-D-thiogalactopyranoside (IPTG). Protein purification was initiated by lysing the cells through extensive sonication, spinning down the insoluble fraction and precipitating the contaminating nucleic acids with addition of 0.15% polyethyleneimine (pH 7.9) dropwise to the lysate at 4°C (38). Precipitate was removed by centrifugation, the supernatant passed over a 10 ml nickel column, and eluted by the addition of 250 mM imidazole. L7Ae containing fractions were exchanged into a 10 mM Na-MES (pH 6.0) buffer and passed over an SP-Sepharose column. The hexahistidine tag was removed with tobacco etch virus (TEV) protease followed by a second round of purification using nickel chromatography.

The gene encoding Nop56/58 homologue (Nop5p) (GI 14590006) was amplified from *P.horikoshii* genomic DNA by PCR and cloned into pET41b (Novagen). The poly-lysine tail of Nop5p (residues 391–403) was deleted from both the wild-type Nop5p and the mNop5p (monomeric Nop5p) proteins; this tail was shown to be unimportant for function (39,40). For mNop5p, the coiled-coil domain was removed (139–242 amino acids). Nop5p and mNop5p proteins contained a glutathione *S*-transferase (GST) tag (41) N-terminal to a hexahistidine affinity tag (42) to enhance solubility. Identical purification protocols were used for both Nop5p and mNop5p using a protocol similar to that for L7ae, except that buffers containing 1 M NaCl were used throughout the purification to enhance the solubility of the protein.

Fibrillarin (GI 14590005) was amplified from *P.horikoshii* genomic DNA by PCR and cloned into ampicillin resistant pET15b. The protein was expressed, the cells lysed and the resultant supernatant collected as for L7Ae (see L7Ae purification). The supernatant was heated to 80°C for 30 min to precipitate non-thermostable proteins. The protein was subsequently purified using a Q-Sepharose column followed by a Sephadex-200 gel filtration column.

RNA synthesis and labeling

RNA was transcribed and purified using standard protocols (43). RNA used in binding studies was labeled with fluorescein at the 3′ end. A total of 100 µg of RNA was used in a 130 µl reaction consisting of 40 mM Na-MES (pH 6.0), 10 mM $MgCl_2$, 5 mM DTT, 10 U CIP and 200 U T4 polynucleotide kinase (44). This mixture was incubated at 37°C for 3 h after which time the RNA was phenol/chloroform extracted and ethanol precipitated. The 3′ vicinal diol was oxidized by resuspending the RNA in 100 µl of freshly made oxidation solution [0.1 M sodium periodate and 0.1 M sodium acetate (pH 5.0)] and incubated at room temperature for 1.5 h in the dark (45). The reaction was quenched by the addition of 11 µl of 2.5 M KCl, placed on ice for 10 min, and the resultant insoluble KIO_4 pellet was removed by a brief centrifugation. A thiosemicarbazide derivative of fluorescein (100 mM in DMSO) was added to a final concentration of 50 mM and incubated at room temperature for 4 h (46). Three phenol/chloroform extractions were performed to remove most of the free fluorophore, the labeled RNA ethanol precipitated, and gel purified by denaturing PAGE.

Electrophoretic mobility shift assays (EMSAs)

Assays to measure the apparent equilibrium dissociation constant (K_d) contained 2 nM fluorophore-labeled RNA in a buffer consisting of 16 mM K-HEPES (pH 7.5), 80 mM KCl, 0.01% NP-40, 2.5 μg tRNA and final protein concentrations ranging from ~0.3 nM to 5 μM. Reactions were allowed to equilibrate on ice for 30 min before loading on native polyacrylamide gels (8%) run in TBE buffer. Gels were imaged on a Typhoon variable mode scanner and the bound and unbound bands quantified. The fraction RNA bound was plotted against protein concentration and the resulting curve was fitted to a Langmuir isotherm

$$\theta = \left(\frac{[\text{protein}]}{[\text{protein}] + K_d}\right)(a - b) + b,$$

where θ is fraction bound, K_d is the apparent dissociation constant, a is the upper baseline and b is the lower baseline. All gel shifts were performed in triplicate and associated error was reported as one standard deviation from the mean.

In vitro methylation experiments

Complexes were assembled in reactions that would yield a final concentration of 10 μM guide/target duplexes. For example, RNAs with two targets were included at 5 μM and single site RNAs were at 10 μM. One mole equivalent of L7Ae, Nop5p and fibrillarin was sequentially added for each box C/D motif present in the RNA. Final buffering conditions for low salt experiments were 10 mM $MgCl_2$, 200 mM KCl and 50 mM K-HEPES (pH 7.5); high salt conditions were 100 mM $MgCl_2$ and 50 mM K-HEPES (pH 7.5) and a defined concentration of KCl ranging from 0.2 to 2.5 M. Tritiated S-adenosylmethionine (76.8 pmols) and cold SAM (38 nmols, 47 μM final concentration) were mixed and added to the assembled complex on ice. The reaction was divided into 30 μl aliquots and incubated at 72°C. At the appropriate time, individual reactions were placed on ice to stop the reaction (data not shown). A total of 25 μl was added to 175 μl of 0.1% trichloroacetic acid (TCA) to precipitate the RNA (47), passed through a nitrocellulose membrane, and washed with 200 μl of TCA. The amount of tritiated SAM incorporated into the RNA was determined using a scintillation counter. Assuming a single turnover reaction, the amount of SAM incorporated versus time was plotted and the data fitted to a first order exponential equation

$$\text{pmols of SAM} = A_0(1 - e^{-kt}) + b,$$

where k is the rate constant for the reaction, t is time in minutes, A_0 is the maximal amount of tritium incorporated and b is a baseline correction. Each experiment was performed in triplicate.

RESULTS

Hemi-complex assembly

Previous work has shown that changing the dimerization interface of Nop5p or the architecture of the sno/sRNA severely reduces or abolishes the activity of the box C/D RNP (23,48), indicating that the architecture is crucial for its ability to act as a methyltransferase. The molecular basis for this loss of activity remains unclear and the affect on methylation specificity has not been addressed. To understand the determinants of activity and specificity, we systematically deconstructed the symmetric archaeal box C/D sRNP. Initially, we created a minimal box C/D complex containing a single guide sequence representing a fully monomeric complex (termed hemi-complex, Figure 1b) by engineering both the Nop5p protein and the box C/D sRNA.

Monomeric Nop5p homolog (referred to as mNop5p henceforth) was created by replacing the coiled-coil domain (139–242 amino acids) with a Gly-Gly-Ala-Gly linker. The crystal structure of the *A.fulgidus* Nop5p/fibrillarin tetrameric complex revealed that dimerization of Nop5p is accomplished entirely by the coiled-coil domain; removal of this domain abrogates dimerization (32). Removing the corresponding sequence from the *P.horikoshii* variant effectively abolished dimer formation as revealed by gel filtration. Full-length Nop5p elutes with a retention volume corresponding to an apparent molecular weight of 127 kDa (true molecular weight for monomer is 45 kDa) consistent with formation of an elongated dimer; mNop5p elutes with an apparent molecular weight of 51 kDa (true molecular weight is 33 kDa) suggesting it behaves as a monomer (Figure 3a). The mixture of mNop5p/fibrillarin (~1:1) yielded two peaks when passed through the sizing column (Figure 3b). The first, which eluted with an apparent molecular weight of 80 kDa, contains both mNop5p and fibrillarin as judged by SDS–PAGE (true molecular weight of 59 kDa for the heterodimer) while the second peak contains only fibrillarin (Figure 3c). Thus, mNop5p retains its ability to specifically bind fibrillarin, indicating that deletion of the coiled-coil has not impaired its ability to productively fold.

The RNA component of our initial hemi-complex was designed with the target sequence covalently attached to the guide region of the box C/D sRNA (Figure 2a). This hemi-RNA contains a consensus box C/D motif with the C and D box sequences of AUGAUGA and CUGA, respectively that define the kink turn motif to which L7Ae binds (24,49,50). L7Ae was readily able to bind this RNA indicating that the core box C/D motif had not been perturbed (Figure 3d). Before assaying the activity and specificity of the hemi-complex, the ability of the complex to assemble as a distinct RNP was investigated. A discrete shift of the hemi-RNA was observed upon each successive addition of L7Ae, mNop5p and fibrillarin (Figure 3d) consistent with observations of the wild-type RNP (31). Thus, the mNop5p construct was shown to be functional with regard to its interactions with fibrillarin and with the L7Ae/box C/D RNA complex as has been shown independently by Maxwell and co-workers (36). Surprisingly, complex assembly did not require elevated assembly temperatures (typically near 70°C) as had been observed in box C/D complexes derived from other thermophilic organisms (23,31). The bands for each assembly step of the box C/D complex were notably cleaner than those seen for the full complex, presumably because of the elimination of conformational heterogeneity in complexes containing the wild-type box C/D RNA (23). This attribute greatly simplifies analysis of the binding affinity of components to the assembling RNP.

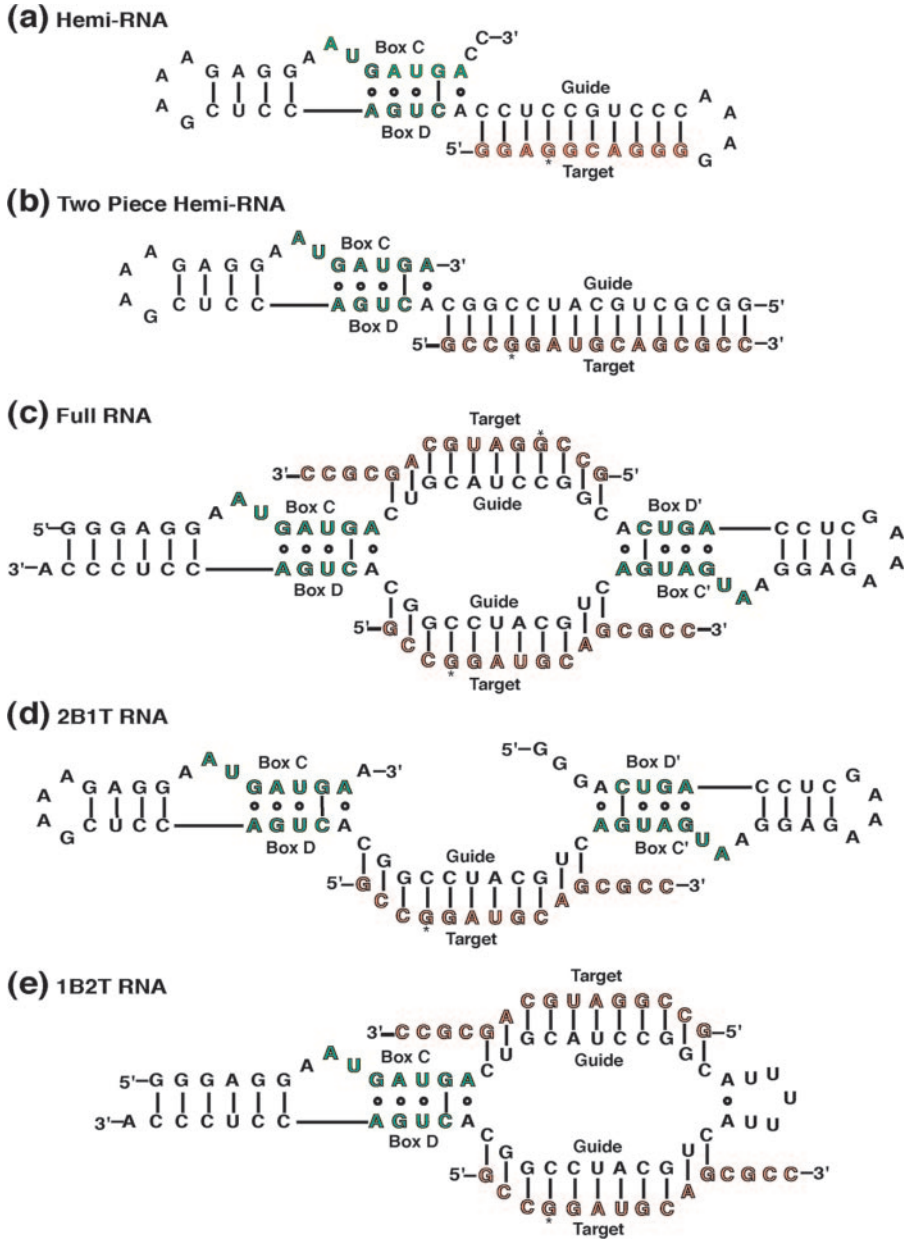

Figure 2. Schematic representations of RNA constructs used. The guide sequence is labeled, the target sequence is labeled and shown in red, and the box C/D and C′/D′ motifs are labeled and shown in green. The site of predicted methylation (five bases upstream from the D or D′ motif) is marked with ∗ for each RNA. (**a**) Hemi-RNA. (**b**) Two piece hemi-RNA. (**c**) Full RNA. (**d**) RNA with two box C/D motifs and one guide sequence. (**e**) RNA with one box C/D motif and two guide sequences.

Hemi-complex gel mobility shifts

Apparent equilibrium dissociation constants (K_d) for assembly were determined by electrophoretic gel mobility shift assays (Table 1). Consistent with previous work (22), L7Ae displays a high affinity for box C/D containing RNA (K_d = 12 ± 5 nM) (Figure 4a and b) while mNop5p binds tightly to the L7Ae/hemi-RNA complex with a K_d of 69 ± 14 nM. The affinity of mNop5p for the hemi-RNA in the absence of L7Ae is 347 ± 47 nM, illustrating the requirement of L7Ae to promote recruitment of mNop5p and implying a stepwise assembly pathway with L7Ae binding to the RNA first followed by Nop5p and fibrillarin or a preassembled Nop5p–fibrillarin complex (31). The mNop5p/fibrillarin dimer has a slightly greater, but reproducible, affinity for the hemi-RNA–L7Ae complex (Figure 4c and d) compared to the affinity of mNop5p alone. This suggests that fibrillarin either interacts with the RNA when positioned properly through association with the hemi-RNA–L7Ae–Nop5p complex or it enhances the affinity of Nop5p for the hemi-RNA–L7Ae complex. The mNop5p/fibrillarin dimer binds only weakly to the hemi-RNA in the absence of L7Ae (K_d = 611 ± 50 nM). Likewise, fibrillarin binds to the hemi-RNA–L7Ae complex with low affinity ($K_d \geqslant$ 500 nM), indicating its interaction with the RNP complex

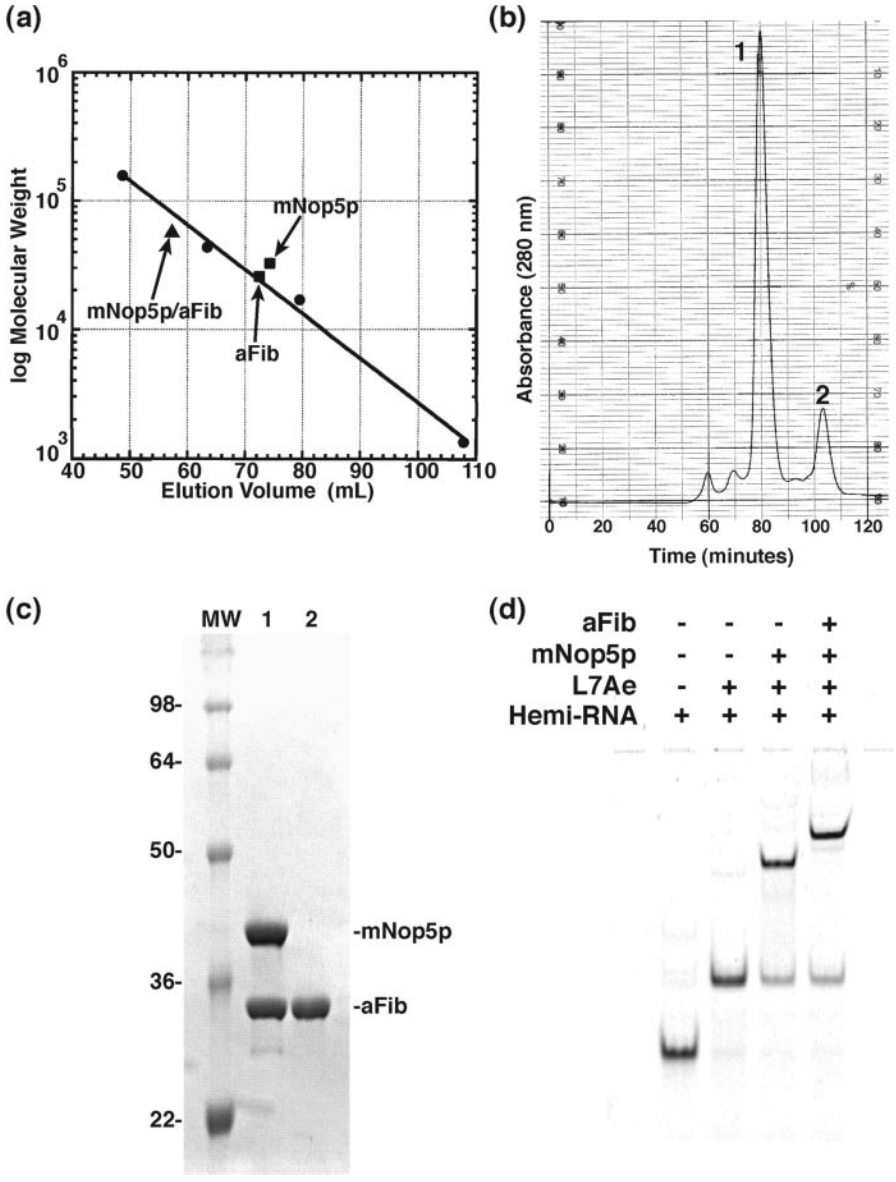

Figure 3. (**a**) Size exclusion chromatography data showing the monomeric state of Nop5p upon removal of the coiled-coil domain. Circles represent size exclusion standards of 1.35, 17, 44 and 158 kDa. (**b**) Size exclusion chromatograph showing that mNop5p is capable of binding to fibrillarin. (**c**) SDS polyacrylamide gel electrophoresis of peaks 1 and 2 from size exclusion data shown in (b). Peak 1 contains mNop5p and fibrillarin while peak 2 contains only fibrillarin. (**d**) Assembly of the box C/D hemi-complex occurs through discrete, well-defined intermediates. Lane 1 shows hemi-RNA (3′ end labeled with Fluorescein). Lane 2 shows hemi-RNA–L7Ae complex. Lane 3 shows hemi-RNA–L7Ae–mNop5p complex. Lane 4 shows hemi-RNA–L7Ae–mNop5p–fibrillarin complex.

is largely mediated through association with mNop5p. The accumulated binding data indicates that our engineering efforts did not adversely affect the ability of the box C/D hemi-complex to assemble through a set of high affinity interactions, clearly demonstrating that the normal protein–RNA and protein–protein interactions have been preserved in the hemi-complex.

Hemi-complex activity

The ability of the hemi-complex to perform the methyl group transfer reaction from *S*-adenosylmethionine to a target strand RNA was investigated by an *in vitro* methylation assay using SAM containing a tritiated methyl group. This method has been previously established as robust and reliable for the detection of methylation activity of box C/D complexes (23,31,48,51). In order to be most sensitive to differences in methylation activity as changes are made to the box C/D complex, the apparent affinity of the hemi-complex for SAM was revealed by determining the degree of methylation as a function of SAM concentration. A titration of wild-type box C/D complex with SAM showed increasing amounts of methylation as the total SAM concentration was increased, with a maximal activity at ≈150 μM (Figure 5a). Fitting this data to a single-site binding model yields an apparent K_d of ≈22 μM, significantly higher than the SAM concentration used in other studies of methylation by the box C/D RNP (23,48). The cellular concentration of SAM in the archaeon

Sulfolobus solfataricus was experimentally found to be between 70 and 90 μM (52), which is on the same order of magnitude as values reported in the literature for a number of eukaryotic tissues (53–55); this result is consistent with these reported intracellular SAM concentrations. For our experiments SAM concentrations were maintained at 50 μM to yield sufficient activity to allow discrimination between partially active and completely inactive complexes.

Initial experiments with the hemi-complex displayed very little methylation activity under previously reported conditions, consistent with prior work on partially asymmetric complexes (23,36,48). However, it was found that the activity exhibited a strong salt dependence. Magnesium ion concentration alone had little effect on activity in the absence of monovalent ions. However, at 3 M monovalent ions we observed significant enhancement in activity in the presence of 50–100 mM magnesium (data not shown). Increasing concentrations of KCl yielded an observed maximal activity at around 2.0 M (Figure 5b). This requirement for elevated salt concentrations for methylation activity is likely due to the removal of the coiled-coil domain from Nop5p for two reasons. First, mNop5p tends to aggregate under low ionic strength conditions but is quite soluble at elevated salt concentrations (data not shown). Second, complexes assembled with hemi-RNA and wild-type Nop5p do not require high salt for activity. The hemi-complex was also found to be most active at temperatures near 75°C (Figure 5c) in agreement with the temperature-activity profile of the wild-type archaeal box C/D RNP (31). The amount of time required for the hemi-complex to achieve maximal methylation (≈10 min) was notably shorter than the times previously observed for wild-type box C/D complexes (⩾40 min). We speculate that this may be in part a consequence of covalent attachment of the target sequence to the hemi-RNA by the GAAA tetraloop. The predicted melting temperature of the guide-target duplex without the GAAA tetraloop is about 50°C whereas the predicted melting temperature of the stem–loop guide-target duplex is 118°C (Mfold) (56) implying that substrate-guide pairing is maintained under the required elevated temperature for reaction (72°C). As we did not want an observed loss of activity to be due to incomplete guide/target annealing in subsequent experiments, care was taken with all constructs to ensure guide/target duplex stability at the temperature required for methylation.

Table 1. Summary of binding data for complexes containing the hemi-RNA construct

Binding data summary	
Hemi-RNA/L7Ae	12 ± 5 nM
(Hemi-RNA/L7Ae)/(mNop5p)	69 ± 14 nM
(Hemi-RNA/L7Ae)/(mNop5p/fibrillarin)	33 ± 6 nM
(Hemi-RNA/L7Ae)/(fibrillarin)	⩾500 nM
Hemi-RNA/mNop5p	347 ± 47 nM
(Hemi-RNA)/(mNop5p/fibrillarin)	611 ± 50 nM

Hemi-complex mismatch intolerance

The wild-type box C/D complex has been shown to be sensitive to mismatched base pairs at the fifth position within the

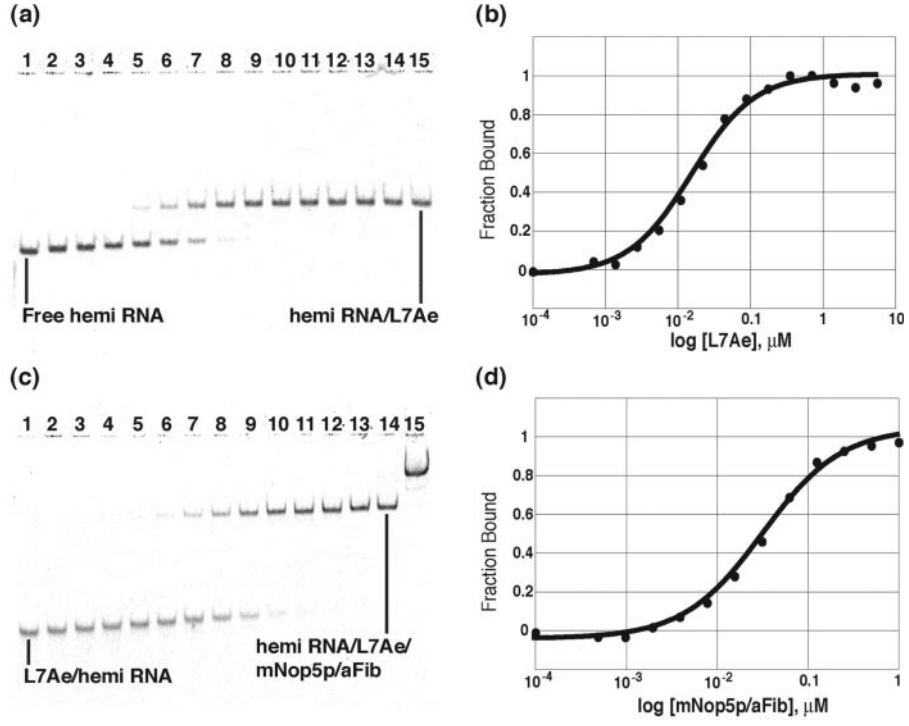

Figure 4. (**a**) Hemi-RNA/L7Ae gel mobility shift. Lane 1 was without L7Ae. L7Ae concentrations for lanes 2–15 ranged from 684 pM to 5.6 μM. Flourescein labeled hemi-RNA was at 2 nM. (**b**) Hemi-RNA/L7Ae binding curve. (K_d for three experiments = 12 ± 5 nM). (**c**) Hemi-RNA-L7Ae/mNop5p-fibrillarin gel mobility shift. Lane 1 was without mNop5p/fibrillarin. Nop/Fib concentrations for lanes 2–15 ranged from 488 pM to 4 μM. Secondary shifts were observed at very high mNop5p concentrations (lane 15) due to higher order complex formation/aggregation. Fluorescein labeled hemi-RNA was at 2 nM. (**d**) Hemi-RNA-L7Ae/mNop5p-fibrillarin binding curve. (K_d for three experiments = 33 ± 6 nM).

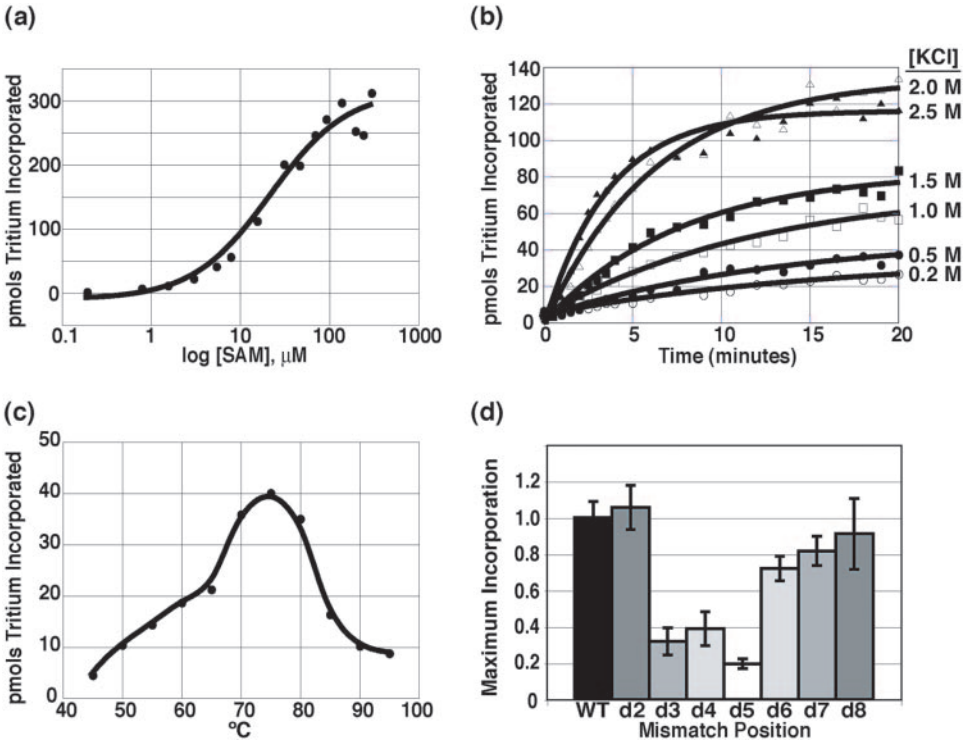

Figure 5. (**a**) Maximum tritium incorporated versus SAM concentration for wild-type box C/D complex. (Apparent $K_d = 22$ μM). (**b**) The activity of the hemi-complex exhibited a strong salt dependence. The salt dependence was explored by increasing the KCl concentration incrementally from 0.2 to 2.5 M and observing the incorporation of tritiated S-adenosylmethionine over time. The magnesium concentration was maintained at 100 mM for all reactions. (**c**) The hemi-complex showed peak activity at ~75°C. (**d**) Non Watson–Crick pairs at positions 3–5 within the target-antisense duplex had pronounced effects on the maximal activity observed for the hemi-complex. Maximum methyl incorporation is shown as fraction of the wild-type value.

guide-target sequence duplex, correlating to the site of 2′-*O*-methylation (31). To investigate this behavior using the hemi-box C/D complex, a series of hemi-RNAs were designed with mismatches at positions 2–8 relative to the box D motif. Mismatches were incorporated into the guide sequence to preserve the 5′-transcription initiation sequence by replacing nucleotides in the guide with the identical nucleotide in the target sequence at each position tested. A mismatch placed at the fifth position in mNop5p complexes showed a significant, although incomplete, drop in activity (Figure 5d). A similar drop in activity occurs when non-Watson–Crick base pairs are present at neighboring positions three and four, while positions further removed from the expected site of methylation were unaffected by non-canonical base pairing. While this result hints at the occurrence of site-specific methylation, it also may reflect sensitivity to structural perturbations of the A-form helix in regions near the methylation site. However, the drop in activity observed is likely not due to changes in duplex stability because of the high melting temperature of the duplex; a single mismatched base pair yields a predicted guide-target melting temperature of 104°C, well above the reaction temperature. In two-piece systems, the decrease in guide-target melting temperature that occurs upon introduction of mismatches could potentially destabilize the duplex enough to account for significant loss of activity in and of itself (i.e. decrease in the activity due to lack of annealing rather than lack of duplex recognition).

The hemi-complex methylates target RNA non-specifically

To more clearly address the specificity of the hemi-complex, a two-piece hemi-box C/D RNA was designed for use with target RNAs containing single 2′-hydroxyl group deletions (Figure 2b). Removal of the 2′-hydroxyl is expected to be minimally disruptive to duplex formation and A-form geometry but completely abrogates the reactive functional group and is therefore ideal for probing site-specific methylation. For instance, target RNA with a single 2′-hydroxyl removed at the fifth position would display no methylation, as observed by transfer of the ^{3}H-methyl group from SAM, if the RNP were completely specific for methylation at that site, as is the wild-type box C/D RNP. Observation of a complete loss of activity upon removal of the position five hydroxyl and minimal loss of activity with the removal of neighboring hydroxyls would thus indicate site-specific methylation. A strong loss of activity at neighboring sites would reflect either deletion of 2′-hydroxyl groups important for protein–RNA interactions or be a result of the complex methylating at that position with some frequency due to loss of fifth position specificity. Targets used for these experiments contain deoxyribose substitutions at positions 3–7 to thoroughly examine specificity.

The ability of the two-piece hemi-complex to specifically methylate its target RNA was examined under elevated salt conditions, as required for activity. Remarkably, removal of the hydroxyl at position five had little effect on the activity

Table 2. Activity data summary for box C/D complex variants

Expt.	Box C/D RNA	Nop	Ionic strength	WT target maximum activity	WT target rate (min^{-1})	Deoxy 3 target maximum activity	Deoxy 4 target maximum activity	Deoxy 5 target maximum activity	Deoxy 6 target maximum activity	Deoxy 7 target maximum activity
A	Hemi-RNA	Mono Nop	High	95 ± 38	0.049 ± 0.002	0.98 ± 0.45	1.12 ± 0.15	0.80 ± 0.26	0.88 ± 0.35	1.22 ± 0.22
B	Full RNA	Full Nop	Low	248 ± 16	0.127 ± 0.025	1.04 ± 0.13	0.83 ± 0.13	0.09 ± 0.04	0.91 ± 0.09	1.08 ± 0.20
C	Hemi-RNA	Full Nop	High	120 ± 29	0.093 ± 0.027	1.16 ± 0.24	1.03 ± 0.33	0.67 ± 0.13	1.25 ± 0.18	1.09 ± 0.30
D	Full RNA	Full Nop	High	214 ± 33	0.306 ± 0.054	1.12 ± 0.37	0.64 ± 0.34	0.14 ± 0.08	0.51 ± 0.24	0.90 ± 0.38
E	Hemi-RNA	Full Nop	Low	144 ± 18	0.044 ± 0.019	0.74 ± 0.13	0.66 ± 0.09	0.37 ± 0.16	0.38 ± 0.03	0.92 ± 0.05
F	Full RNA	Mono Nop	High	130 ± 29	0.062 ± 0.023	0.73 ± 0.17	0.60 ± 0.25	0.33 ± 0.15	0.79 ± 0.19	0.85 ± 0.28
G	2B1T RNA	Full Nop	Low	158 ± 12	0.163 ± 0.010	0.84 ± 0.11	0.72 ±0.07	0.14	0.78 ± 0.15	0.77 ± 0.14
H	1B2T RNA	Full Nop	Low	287 ± 54	0.078 ± 0.061	0.70	0.48 ± 0.3	0.40 ± 0.04	0.41 ± 0.17	0.61 ± 0.03

The activity with deoxy targets 3–7 for each complex is represented as fractions of wild-type target activity for that same complex. High ionic strength conditions had 2.0 M KCl and 100 mM $MgCl_2$. Low ionic strength conditions had 0.2 M KCl and 10 mM $MgCl_2$.

of the complex relative to its ability to methylate a control RNA containing no deoxy substitutions (Table 2, expt. A), indicating the hemi-complex methylates the RNA at other sites. To determine if the site of methylation shifted to another 2′-hydroxyl, targets with deoxys at neighboring positions 3–7 were tested. No significant drop in activity was observed for any of these target RNAs. Furthermore, a target RNA with three 2′-hydroxyls removed from positions 4–6 exhibits only a slight decrease in activity (data not shown). In contrast, performing the same experiment with an RNA containing both the box C/D and C′/D′ kink-turn motifs (Figure 2c) under low salt concentrations results in a complete loss of activity when the 2′-hydroxyl at position five was removed while the activity was unaffected by removing any other 2′-hydroxyl groups between positions 3 and 7 as expected for wild-type complexes (Table 2, expt. B). The full RNA contained a canonical K-turn motif at the C′/D′ position rather than the single stem K-loop observed in *Pyrococcus* box C/D RNAs (25). Clearly, the hemi-complex is competent to methylate RNA, but completely non-specific with respect to the position of methylation; conceivably this enzyme could also be methylating the guide strand as well.

The complete loss of specificity observed in the hemi-complex could be caused by a combination of the three alterations made to the wild-type box C/D complex. First, it may be the result of the removal of the coiled-coil domain from Nop5p. Second, the high salt conditions necessary for hemi-complex activity may abrogate specificity by interfering with important protein–RNA contacts and the ability of fibrillarin to align with the guide-target duplex. Finally, the hemi-RNA itself may lack a specificity-conferring quality present in full box C/D RNAs. With these possibilities in mind, we began a systematic reconstruction of the full box C/D complex to identify the component that when restored rescues pinpoint specificity to determine the principal contributors to specificity.

Specificity is largely imparted by the RNA component

In the first step towards understanding specificity, a complex consisting of wild-type Nop5p and the two-piece hemi-RNA (Figure 2b) was assembled to test the effect of coiled-coil removal. The salt concentration was kept at 2 M to allow for direct comparison with mNop5p results. This complex displays a lack of specificity as evidenced by the significant activity seen for targets with a 2′-hydroxyl removed from position 3–7 (Figure 6a and Table 2, expt. C), as observed with the hemi-complex. Therefore, removal of the coiled-coil domain from Nop5p does not account for the loss of specificity observed in the hemi-complex.

To test the effect of high salt on specificity, full RNA complexes were assembled with full Nop5p at 2.0 M KCl and 100 mM $MgCl_2$. This complex exhibits an increase in specificity levels as evidenced by a further decrease in the activity observed for position five-hydroxyl removal (Figure 6b and Table 2, expt. D). However, sensitivity to hydroxyl removal at neighboring positions 4 and 6 is present. Decreasing salt concentration to physiological levels (200 mM) alleviates the slight loss of methylation competency occuring upon removal of these neighboring hydroxyls (Table 2, expt. B). The requirement for the presence of flanking 2′-hydroxyls at high ionic strength may be due to a weakening of electrostatic interactions between RNA and Nop5p/fibrillarin, which would increase the importance of hydrogen bonding with 2′-hydroxyl groups. Thus, elevated ionic strength does not account for the loss of specificity observed although a small increase in specificity was seen for hemi-RNA complexes with full Nop under low ionic strength conditions (Table 2, expt. E).

Since neither restoration of the coiled-coil domain and Nop5p dimerization nor lowering ionic strength re-established specificity, the role of the RNA was investigated (Figure 6c). Compared to the hemi-complexes, RNPs assembled with full RNA and mNop5p under high salt conditions (2.0 M) demonstrate a dramatic improvement in methylation specificity (Figure 6c and Table 2, expt. F). However, this complex differed from the wild-type complex under physiological conditions in that a residual amount of activity was retained with removal of the fifth position hydroxyl. Also, sensitivity to removal of neighboring hydroxyls was observed. This is likely due to the elevated salt concentrations since wild-type complexes at 2 M salt exhibited the same sensitivity at neighboring positions while no such effect was seen at 0.2 M salt concentrations. Thus, the RNA component of box C/D complexes is the most significant contributor to site-specific methylation.

An asymmetric RNA exhibits wild-type specificity

It is well established that the site of methylation within box C/D targets is in part dictated by a spacing of five bases 3′ of either the D or the D′ boxes (20). However, our data

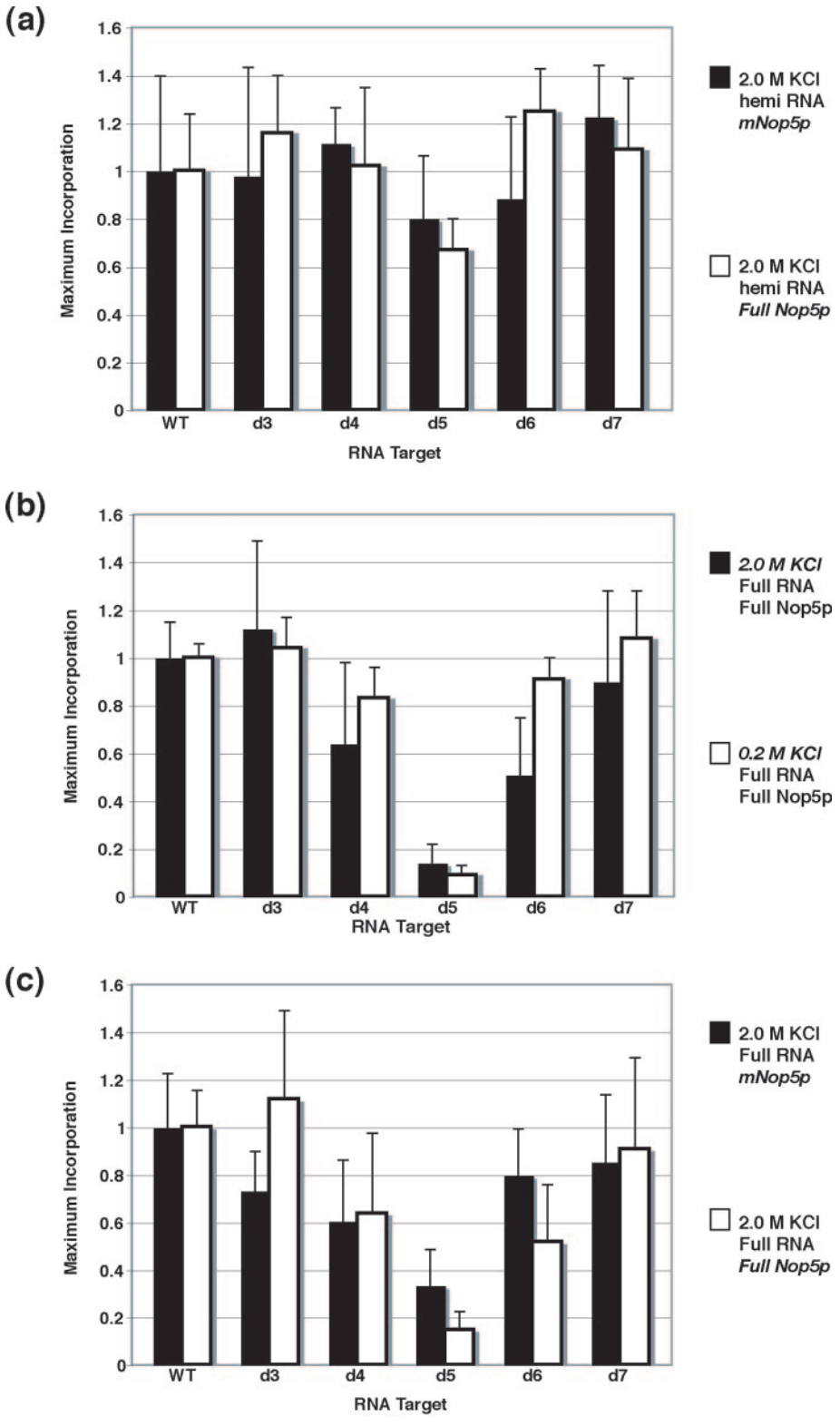

Figure 6. Tritium incorporation with various deoxy containing RNA targets under varying conditions. (**a**) A comparison between complexes set up with the hemi-RNA, L7Ae, mNop5p and fibrillarin (Black) and complexes set up with the hemi-RNA, L7Ae, Full Nop5p and fibrillarin (White). Both reactions were conducted at 2 M KCl, 100 mM $MgCl_2$. Restoration of coiled coil domain in Nop5p does not impart specificity in half RNA complexes. (**b**) A comparison between complexes set up with the full RNA, L7Ae, Full Nop5p and fibrillarin (Black) at 2.0 M KCl, 100 mM $MgCl_2$ and complexes set up with the full RNA, L7Ae, Full Nop5p and fibrillarin (White) at 0.2 M KCl, 10 mM $MgCl_2$. Increased KCl and $MgCl_2$ concentration does not significantly alter specificity. (**c**) A comparison between complexes set up with the full RNA, L7Ae, mNop5p and fibrillarin (Black) and complexes set up with the full RNA, L7Ae, Full Nop5p and fibrillarin (White). Both reactions were conducted at 2 M KCl, 100 mM $MgCl_2$. Restoration of Full RNA imparts significant specificity in both full and mNop5p complexes.

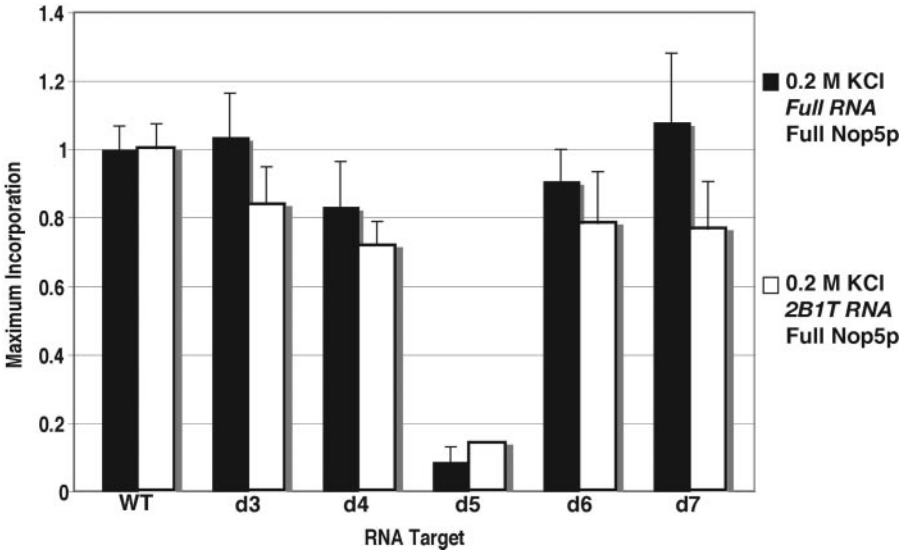

Figure 7. A comparison between complexes set up with the full RNA, L7Ae, full Nop5p and fibrillarin (Black) and complexes set up with the 2B1T RNA, L7Ae, Full Nop5p and fibrillarin (White). Both reactions were conducted at 0.2 M KCl, 10 mM $MgCl_2$. Target RNAs used were either unaltered 'wild-type' (WT), or contained single 2′-hydroxyl deoxy substitutions at positions 3–7 upstream from the D box motif (designated d3–d7). Wild-type specificity is achieved with an asymmetric RNA containing a C′/D′ motif but devoid of a D′ directed targeting sequence.

strongly suggests that a further contributor of specificity is tethering of the RNA to the box C′/D′ motif. The proposed Nop5p dimer could potentially span the distance between the two L7Ae/kink turn complexes creating a bowed structure that positions the appropriate 2′-hydroxyl against the fibrillarin active site, locking the target/guide duplex into place for methylation, compensating for the relatively weak affinity of fibrillarin for dsRNA. This line of thought lead to the hypothesis that two box C/D motifs are required to achieve specificity but not two guide sequences. To test this, an RNA was designed with two box C/D motifs but only one targeting sequence (2B1T) (Figure 2d) and assayed for site-specific methylation when complexed with Nop5p under physiological salt concentrations. Like the full RNA construct, this RNA contained a canonical two stem K-turn motif at the box C′/D′ position. These experiments yield a specificity profile virtually identical to the wild-type box C/D complex (Figure 7 and Table 2, expt. G), reinforcing the idea that the box C′/D′ motif is contributing to the specificity of a C/D positioned target through protein–RNA interactions. Interestingly, complexes set up with the 2B1T RNA and mNop5p exhibited a lack of specificity similar to that seen for the hemi-complex (data not shown) demonstrating a context-dependent effect on specificity with coiled-coil domain removal. As a further test, an RNA containing only one box C/D motif but two guide sequences (Figure 2e) was constructed in which the two targeting sequences were joined by a five uracil linker in place of the C′/D′ motif. This one box C/D two target RNA (1B2T) was active under physiological conditions with full Nop5p. However, while the activity of this complex when used with target RNA with the fifth position hydroxyl removed was significantly down from wild-type target, there was still a significant amount of activity, similar to what was seen in the highly non-specific hemi-complexes (Table 2, expt. H). Also, removal of hydroxyls at neighboring positions resulted in a clear drop in activity yet none of the targets were seen to completely abolish activity. This implies that the 1B2T RNA is not capable of site-specifically methylating RNA targets. Thus, both box C/D motifs are required for the archaeal sRNP to achieve full specificity but only one guide sequence.

DISCUSSION

The structural requirements for specificity and activity in box C/D sno/sRNPs have only been partially defined. To date, the primary determinant for site-specific methylation that has been revealed is a strict adherence to the N + 5 rule (20). This rule states that 2′-hydroxyl methylation occurs within the target RNA strand at the nucleotide paired to the guide sequence 5 nt 5′ of either the D or D′ box. This implies that specificity occurs through a ruler-like mechanism in which fibrillarin is correctly positioned over the site of methylation through association with proteins (L7Ae and Nop5p), which bind to the box C/D or C′/D′ motifs in a highly specific manner. However, given the complex architecture of this RNP enzyme, there are likely other structural requirements that confer site-specificity to fibrillarin, which is inherently non-specific.

Related to this issue is the symmetric nature of archaeal box C/D complexes that has been shown to be important for activity for reasons that remain unclear. An asymmetric complex composed of a single box C/D motif, L7Ae, Nop5p and fibrillarin could conceivably carry out site-specific methylation, however, previous work demonstrated a functional requirement for symmetry in box C/D complexes with partially asymmetric complexes exhibiting dramatically reduced activity (23,48). In these studies, we demonstrate that the bipartite architecture of the box C/D sRNP is essential for site-specific methylation, accounting for the absolutely conserved pseudo-symmetric architecture in naturally occurring

complexes, but not for intrinsic methylation activity. Specifically, we demonstrate that both the box C/D and box C′/D′ motifs are required for pinpoint specificity.

The relationship between architectural symmetry, activity and the specificity of a model box C/D sRNP derived from *P.horikoshii* was explored through a reductive approach in which the box C/D sRNP was systematically disassembled from a symmetric complex to a fully asymmetric one. This approach revealed the relative importance of structural components in the context of both reduced and otherwise wild-type complexes. Strikingly, the fully reduced complex (hemi-RNP) displays most of the same features and activity of the wild-type complex including its ability to assemble into tight, well-defined intermediary complexes exhibiting binding affinities in accord with those observed for fully functional structurally intact box C/D complexes (23,32). Additionally, contrary to previous observations, the completely asymmetric hemi-complex was found to be quite active, exhibiting a temperature dependent activity profile identical to what has been observed with wild-type box C/D complexes (31). However, removal of the coiled-coil domain of Nop5p introduced a strong salt requirement for activity, with methylation being restored only under high salt concentrations. Thus, while it has been proposed that the coiled-coil domain of Nop5p enables cross talk between the two active sites (23), we have demonstrated that this is not required for activity. Aside from the salt requirement, the inability of other studies to detect significant levels of methyl incorporation with asymmetric complexes may also have been due to the use of insufficient SAM concentrations (23,48). A SAM titration with a wild-type box C/D complex revealed an optimal SAM concentration well above the amount used in previous studies and more aligned with physiological SAM concentrations of 20–100 μM (52–55).

The key difference between the wild-type RNP and the hemi-complex is that the latter exhibits a complete loss of specificity. This loss is not due to removal of the coiled-coil domain since hemi-RNA assembled with full Nop5p under both low and high salt concentrations is largely unable to site specifically methylate their target RNAs. Instead, a significant increase in specificity occurs in complexes with the full RNA regardless of the use of mNop5p, full Nop5p, high or low salt concentrations. These data demonstrate the importance of RNA structure distal to the methyl-directing C/D motif, further supported by using an RNA with a single box C/D motif but containing two guide sequences joined by a poly(U) linker in place of the C′/D′ motif. When incorporated into full Nop5p complexes under low salt conditions, this RNA was fully non-specific, mimicking the properties of the hemi-RNA. On the other hand, an RNA containing a single guide sequence but possessing both C/D and C′/D′ motifs was able to direct methylation with wild-type specificity. Therefore, the simple addition of a second box C/D motif to the hemi-RNA construct took us from a completely nonspecific complex to a highly specific methyltransferase. This asymmetric RNA reveals much about the requirement for bipartite structure (C/D and C′/D′ motifs) in the highly specific box C/D sRNPs and reflects the ability of eukaryotic box C/D RNAs with only one functional guide sequence to function as single site enzymes (16). The crystal structure of the Nop5p/fibrillarin tetramer (32) revealed that the fibrillarin active sites appear to be too far apart for simultaneous methylation at both targets (36). Our results suggest that only one active site might be productively used at a time in the wild-type complex, consistent with observations made by Maxwell and coworkers (36).

A comparison of residues within the coiled-coil domain region between *A.fulgidus* and representative eukaryotes is highly suggestive of a eukaryotic Nop56p/Nop58p dimer (32) although the interaction is speculative with recent work showing that Nop56p/Nop58p self-dimerization and the interaction of Nop56p/Nop58p with fibrillarin are mutually exclusive protein–protein interactions in *Methanocaldococcus jannaschii* (36). Our work demonstrates that dimerization of Nop5p in full RNA complexes is not necessary for specificity or activity. However, Nop5p dimerization through the coiled-coil domain was shown to be important for specificity in the context of the 2B1T RNA suggesting that the wild-type box C/D sRNA structure can overcome the need for the proposed dimerization of Nop5p but that this dimerization may still be important in more structurally deviant single guide snoRNA–sRNA complexes similar to the 2B1T RNA. It is tempting to speculate that an insertion sequence of ~60 amino acids between the two alpha helices of the Nop5p coiled-coil serves to anchor this protein to the second box C/D element through protein–protein or protein–RNA interactions that might be especially critical in the 2B1T RNA lacking the second guide sequence.

The coiled coil domain of Nop5p undoubtedly contributes to proper guide/target duplex positioning for pinpoint specificity; this role is supported by previous work as well as the data presented here. However, it also clear that the sRNA plays a dominant role in organizing the RNP and directing fibrillarin to the correct site of methylation. A recent study by Omer and coworkers in which the box C/D RNA of *S.solfataricus* was extensively probed using site-directed mutagenesis and tested for methylation activity supports this view (57). Taken together our data reinforces the importance of the bipartite structure seen in archaeal and eukaryal box C/D complexes whose primary function is to deliver a specific 2′-hydroxyl group to an active site that is potentially capable of recognizing any dsRNA.

ACKNOWLEDGEMENTS

The authors would like to thank Jeffrey Kieft, Johnny Croy, Sunny Gilbert, Rebecca Montange and Colby Stoddard for critically reading this manuscript and the members of the Batey laboratory for critical discussions. Matthew Grantz, Elizabeth Pleshe and Diane Starrett provided technical assistance at various phases of this project. This work was supported by the W. M. Keck Foundation and through startup funds provided by the University of Colorado, Boulder. Funding to pay the Open Access publication charges for this article was provided by W. M. Keck Foundation.

Conflict of interest statement. None declared.

REFERENCES

1. Rozenski,J., Crain,P.F. and McCloskey,J.A. (1999) The RNA Modification Database: 1999 update. *Nucleic Acids Res.*, **27**, 196–197.

2. Sprinzl,M., Horn,C., Brown,M., Ioudovitch,A. and Steinberg,S. (1998) Compilation of tRNA sequences and sequences of tRNA genes. *Nucleic Acids Res*., **26**, 148–153.
3. Ziesche,S.M., Omer,A.D. and Dennis,P.P. (2004) RNA-guided nucleotide modification of ribosomal and non-ribosomal RNAs in Archaea. *Mol. Microbiol*., **54**, 980–993.
4. Clouet-d'Orval,B., Gaspin,C. and Mougin,A. (2005) Two different mechanisms for tRNA ribose methylation in Archaea: a short survey. *Biochimie*, **87**, 889–895.
5. Decatur,W.A. and Fournier,M.J. (2003) RNA-guided nucleotide modification of ribosomal and other RNAs. *J. Biol. Chem*., **278**, 695–698.
6. Kiss,T. (2001) Small nucleolar RNA-guided post-transcriptional modification of cellular RNAs. *EMBO J*., **20**, 3617–3622.
7. Decatur,W.A. and Fournier,M.J. (2002) rRNA modifications and ribosome function. *Trends Biochem. Sci*., **27**, 344–351.
8. Peculis,B.A. (1997) The sequence of the 5′ end of the U8 small nucleolar RNA is critical for 5.8S and 28S rRNA maturation. *Mol. Cell. Biol*., **17**, 3702–3713.
9. Tycowski,K.T., Shu,M.D. and Steitz,J.A. (1994) Requirement for intron-encoded U22 small nucleolar RNA in 18S ribosomal RNA maturation. *Science*, **266**, 1558–1561.
10. Sirum-Connolly,K. and Mason,T.L. (1995) The role of nucleotide modifications in the yeast mitochondrial ribosome. *Nucleic Acids Symp. Ser*., **33**, 73–75.
11. Sirum-Connolly,K. and Mason,T.L. (1993) Functional requirement of a site-specific ribose methylation in ribosomal RNA. *Science*, **262**, 1886–1889.
12. Cunningham,P.R., Richard,R.B., Weitzmann,C.J., Nurse,K. and Ofengand,J. (1991) The absence of modified nucleotides affects both *in vitro* assembly and *in vitro* function of the 30S ribosomal subunit of *Escherichia coli*. *Biochimie*, **73**, 789–796.
13. Helm,M. (2006) Post-transcriptional nucleotide modification and alternative folding of RNA. *Nucleic Acids Res*., **34**, 721–733.
14. Dennis,P.P., Omer,A. and Lowe,T. (2001) A guided tour: small RNA function in Archaea. *Mol. Microbiol*., **40**, 509–519.
15. Omer,A.D., Lowe,T.M., Russell,A.G., Ebhardt,H., Eddy,S.R. and Dennis,P.P. (2000) Homologs of small nucleolar RNAs in Archaea. *Science*, **288**, 517–522.
16. Kiss-Laszlo,Z., Henry,Y., Bachellerie,J.P., Caizergues-Ferrer,M. and Kiss,T. (1996) Site-specific ribose methylation of preribosomal RNA: a novel function for small nucleolar RNAs. *Cell*, **85**, 1077–1088.
17. Tycowski,K.T., Smith,C.M., Shu,M.D. and Steitz,J.A. (1996) A small nucleolar RNA requirement for site-specific ribose methylation of rRNA in *Xenopus*. *Proc. Natl Acad. Sci. USA*, **93**, 14480–14485.
18. Gaspin,C., Cavaille,J., Erauso,G. and Bachellerie,J.P. (2000) Archaeal homologs of eukaryotic methylation guide small nucleolar RNAs: lessons from the *Pyrococcus* genomes. *J. Mol. Biol*., **297**, 895–906.
19. Tran,E., Zhang,X., Lackey,L. and Maxwell,E.S. (2005) Conserved spacing between the box C/D and C′/D′ RNPs of the archaeal box C/D sRNP complex is required for efficient 2′-O-methylation of target RNAs. *RNA*, **11**, 285–293.
20. Omer,A.D., Ziesche,S., Decatur,W.A., Fournier,M.J. and Dennis,P.P. (2003) RNA-modifying machines in archaea. *Mol. Microbiol*., **48**, 617–629.
21. Kuhn,J.F., Tran,E.J. and Maxwell,E.S. (2002) Archaeal ribosomal protein L7 is a functional homolog of the eukaryotic 15.5 kD/Snu13p snoRNP core protein. *Nucleic Acids Res*., **30**, 931–941.
22. Rozhdestvensky,T.S., Tang,T.H., Tchirkova,I.V., Brosius,J., Bachellerie,J.P. and Huttenhofer,A. (2003) Binding of L7Ae protein to the K-turn of archaeal snoRNAs: a shared RNA binding motif for C/D and H/ACA box snoRNAs in Archaea. *Nucleic Acids Res*., **31**, 869–877.
23. Tran,E.J., Zhang,X. and Maxwell,E.S. (2003) Efficient RNA 2′-O-methylation requires juxtaposed and symmetrically assembled archaeal box C/D and C′/D′ RNPs. *EMBO J*., **22**, 3930–3940.
24. Szewczak,L.B., Gabrielsen,J.S., Degregorio,S.J., Strobel,S.A. and Steitz,J.A. (2005) Molecular basis for RNA kink-turn recognition by the h15.5K small RNP protein. *RNA*, **11**, 1407–1419.
25. Nolivos,S., Carpousis,A.J. and Clouet-d'Orval,B. (2005) The K-loop, a general feature of the *Pyrococcus* C/D guide RNAs, is an RNA structural motif related to the K-turn. *Nucleic Acids Res*., **33**, 6507–6514.
26. Suryadi,J., Tran,E.J., Maxwell,E.S. and Brown,B.A.,2nd (2005) The crystal structure of the *Methanocaldococcus jannaschii* multifunctional L7Ae RNA-binding protein reveals an induced-fit interaction with the box C/D RNAs. *Biochemistry*, **44**, 9657–9672.
27. Moore,T., Zhang,Y., Fenley,M.O. and Li,H. (2004) Molecular basis of box C/D RNA-protein interactions; cocrystal structure of archaeal L7Ae and a box C/D RNA. *Structure*, **12**, 807–818.
28. Aittaleb,M., Visone,T., Fenley,M.O. and Li,H. (2004) Structural and thermodynamic evidence for a stabilizing role of Nop5p in S-adenosyl-L-methionine binding to fibrillarin. *J. Biol. Chem*., **279**, 41822–41829.
29. Deng,L., Starostina,N.G., Liu,Z.J., Rose,J.P., Terns,R.M., Terns,M.P. and Wang,B.C. (2004) Structure determination of fibrillarin from the hyperthermophilic archaeon *Pyrococcus furiosus*. *Biochem. Biophys. Res. Commun*., **315**, 726–732.
30. Wang,H., Boisvert,D., Kim,K.K., Kim,R. and Kim,S.H. (2000) Crystal structure of a fibrillarin homologue from *Methanococcus jannaschii*, a hyperthermophile, at 1.6 A resolution. *EMBO J*., **19**, 317–323.
31. Omer,A.D., Ziesche,S., Ebhardt,H. and Dennis,P.P. (2002) *In vitro* reconstitution and activity of a C/D box methylation guide ribonucleoprotein complex. *Proc. Natl Acad. Sci. USA*, **99**, 5289–5294.
32. Aittaleb,M., Rashid,R., Chen,Q., Palmer,J.R., Daniels,C.J. and Li,H. (2003) Structure and function of archaeal box C/D sRNP core proteins. *Nature Struct. Biol*., **10**, 256–263.
33. Hamma,T. and Ferre-D'Amare,A.R. (2004) Structure of protein L7Ae bound to a K-turn derived from an archaeal box H/ACA sRNA at 1.8 A resolution. *Structure*, **12**, 893–903.
34. Szewczak,L.B., DeGregorio,S.J., Strobel,S.A. and Steitz,J.A. (2002) Exclusive interaction of the 15.5 kD protein with the terminal box C/D motif of a methylation guide snoRNP. *Chem. Biol*., **9**, 1095–1107.
35. Cahill,N.M., Friend,K., Speckmann,W., Li,Z.H., Terns,R.M., Terns,M.P. and Steitz,J.A. (2002) Site-specific cross-linking analyses reveal an asymmetric protein distribution for a box C/D snoRNP. *EMBO J*., **21**, 3816–3828.
36. Zhang,X., Champion,E.A., Tran,E.J., Brown,B.A.,2nd, Baserga,S.J. and Maxwell,E.S. (2006) The coiled-coil domain of the Nop56/58 core protein is dispensable for sRNP assembly but is critical for archaeal box C/D sRNP-guided nucleotide methylation. *RNA*, **12**, 1092–1103.
37. Sambrook,J. and Russell,D.W. (2001) *Molecular Cloning: A Laboratory Manual*, 3rd ed. Cold Spring Harbor Laboratory Press, Cold Spring Harbor, NY.
38. Kirk,N. and Cowan,D. (1995) Optimising the recovery of recombinant thermostable proteins expressed in mesophilic hosts. *J. Biotechnol*., **42**, 177–184.
39. Lafontaine,D.L. and Tollervey,D. (1999) Nop58p is a common component of the box C+D snoRNPs that is required for snoRNA stability. *RNA*, **5**, 455–467.
40. Lafontaine,D.L. and Tollervey,D. (2000) Synthesis and assembly of the box C+D small nucleolar RNPs. *Mol. Cell. Biol*., **20**, 2650–2659.
41. Lichty,J.J., Malecki,J.L., Agnew,H.D., Michelson-Horowitz,D.J. and Tan,S. (2005) Comparison of affinity tags for protein purification. *Protein Expr. Purif*., **41**, 98–105.
42. Terpe,K. (2003) Overview of tag protein fusions: from molecular and biochemical fundamentals to commercial systems. *Appl. Microbiol. Biotechnol*., **60**, 523–533.
43. Doudna,J.A. (1997) Preparation of homogeneous ribozyme RNA for crystallization. *Meth. Mol. Biol*., **74**, 365–370.
44. Cameron,V. and Uhlenbeck,O.C. (1977) 3′-Phosphatase activity in T4 polynucleotide kinase. *Biochemistry*, **16**, 5120–5126.
45. Qin,P.Z. and Pyle,A.M. (1999) Site-specific labeling of RNA with fluorophores and other structural probes. *Methods*, **18**, 60–70.
46. Wu,T.P., Ruan,K.C. and Liu,W.Y. (1996) A fluorescence-labeling method for sequencing small RNA on polyacrylamide gel. *Nucleic Acids Res*., **24**, 3472–3473.
47. Nau,F. and Pham-Coeur-Joly,G. (1981) tRNA methylation. A rapid and simple method for determination of total radioactivity and methylated base distribution in the same sample. *Biochim. Biophys. Acta*, **653**, 299–302.
48. Rashid,R., Aittaleb,M., Chen,Q., Spiegel,K., Demeler,B. and Li,H. (2003) Functional requirement for symmetric assembly of archaeal box C/D small ribonucleoprotein particles. *J. Mol. Biol*., **333**, 295–306.
49. Klein,D.J., Schmeing,T.M., Moore,P.B. and Steitz,T.A. (2001) The kink-turn: a new RNA secondary structure motif. *EMBO J*., **20**, 4214–4221.

50. Matsumura,S., Ikawa,Y. and Inoue,T. (2003) Biochemical characterization of the kink-turn RNA motif. *Nucleic Acids Res*., **31**, 5544–5551.
51. Bortolin,M.L., Bachellerie,J.P. and Clouet-d'Orval,B. (2003) *In vitro* RNP assembly and methylation guide activity of an unusual box C/D RNA, *cis*-acting archaeal pre-tRNA(Trp). *Nucleic Acids Res*., **31**, 6524–6535.
52. Porcelli,M., Cacciapuoti,G., Carteni-Farina,M. and Gambacorta,A. (1988) S-adenosylmethionine synthetase in the thermophilic archaebacterium *Sulfolobus solfataricus*. Purification and characterization of two isoforms. *Eur. J. Biochem*., **177**, 273–280.
53. Martinov,M.V., Vitvitsky,V.M., Mosharov,E.V., Banerjee,R. and Ataullakhanov,F.I. (2000) A substrate switch: a new mode of regulation in the methionine metabolic pathway. *J. Theor. Biol*., **204**, 521–532.
54. Huang,Z.Z., Mao,Z., Cai,J. and Lu,S.C. (1998) Changes in methionine adenosyltransferase during liver regeneration in the rat. *Am. J. Physiol*., **275**, G14–G21.
55. Lu,S.C., Gukovsky,I., Lugea,A., Reyes,C.N., Huang,Z.Z., Chen,L., Mato,J.M., Bottiglieri,T. and Pandol,S.J. (2003) Role of S-adenosylmethionine in two experimental models of pancreatitis. *FASEB J*., **17**, 56–58.
56. Zuker,M. (2003) Mfold web server for nucleic acid folding and hybridization prediction. *Nucleic Acids Res*., **31**, 3406–3415.
57. Omer,A.D., Zago,M., Chang,A. and Dennis,P.P. (2006) Probing the structure and function of an archaeal C/D-box methylation guide sRNA. *RNA*.